Wind and Structures, *Vol. 30, No. 2 (2020) 165-180*
DOI: https://doi.org/10.12989/was.2020.30.2.165

Influence of a community of buildings on tornadic wind fields

Zhi Li[1], Ryan Honerkamp[1], Guirong Yan*[1] and Ruoqiang Feng[2]

[1]*Department of Civil, Architectural and Environmental Engineering, Missouri University of Science and Technology, 1401 Pine St, Rolla, MO 65409*
[2] *Structural Engineering Service Dept., Sumitomo Mitsui Construction co., ltd., Tsukuda, Chuou-ku, Tokyo 104-0051, Japan*

(Received January 10, 2018, Revised July 8, 2019, Accepted September 17, 2019)

Abstract. To determine tornadic wind loads, the wind pressure, forces and moments induced by tornadoes on civil structures have been studied. However, in most previous studies, only the individual building of interest was included in the wind field, which may be suitable to simulate the case where a tornado strikes rural areas. The statistical data has indicated that tornadoes induce more significant fatalities and property loss when they attack densely populated areas. To simulate this case, all buildings in the community of interest should be included in the wind field. However, this has been rarely studied. To bridge this research gap, this study will systematically investigate the influence of a community of buildings on tornadic wind fields by modeling all buildings in the community into the wind field (designated as "the Community case under tornadic winds"). For comparison, the case in which only a single building is included in the tornadic wind field (designated as "the Single-building case under tornadic winds") and the case where a community of buildings are included in the equivalent straight-line wind field (designated as "the Community case under straight-line winds") are also simulated. The results demonstrate that the presence of a number of buildings completely destroys the pattern of regular circular strips in the distribution of tangential velocity and pressure on horizontal planes. Above the roof height, the maximum tangential velocity is lower in the Community case under tornadic winds than that in the Single-building case under tornadic winds because of the higher surface friction in the Community case; below the roof height, greater tangential velocity and pressure are observed in the Community case under tornadic wind fields, and more unfavorable conditions are observed in the Community case under tornadic winds than under the equivalent straight-line winds.

Keywords: translating tornadic wind fields; computational fluid dynamics; gable-roofed buildings; straight-line wind

1. Introduction

In reality, in urban populated areas, a civil structure is always surrounded by other structures. When tornadoes strike this type of area, the presence of the surrounding structures may affect the tornadic wind field, which in turn may affect the wind pressure induced on the structure of interest by tornadoes. To properly determine the tornadic wind load, it is important to investigate how the surrounding structures affect the tornadic wind flow by modelling the surrounding structures in the computational domain in addition to the structure of interest. Although the influence of the presence of surrounding structures on the straight-line wind fields has been widely studied, Khanduri *et al.* (1998), Nozawa and Tamura (2002), Chang and Meroney (2003), Xie and Gu (2004), Lam *et al.* (2008, 2011), Wang *et al.* (2014), Blocken *et al.* (2016) and Elshaer *et al.* (2016), the influence of surrounding structures on tornadic wind fields is still unknown.

Some previous studies did investigate the influence of surface roughness of the ground on the tornadic wind field in laboratory tornado simulators by modeling surface roughness using rectangular blocks or other shapes of obstruction. Dessens (1972) attached sharp edged pebbles, measuring 6-mm in diameter, to the surface of a wood plate to replicate roughness. He compared two cases, a tornado-like vortex passing over a surface with and without roughness. He concluded that increasing surface roughness enlarged the core radius and the maximum vertical velocity but decreased the maximum tangential velocity. This is consistent with the later laboratory simulation results by Wilkins *et al.* (1975). Leslie (1977) placed a shag carpet, with a fiber length of 2.54 cm, on the surface to generate roughness, which was chosen because it produced a boundary layer similar to the atmospheric boundary layer in straight-line wind tunnels. He concluded that surface roughness increased the magnitude of swirl ratio and made the flow more turbulent. Based on the present authors' simulation results, the swirl ratio is directly related to the core radius. To be specific, the higher swirl ratio, the higher the core radius. Therefore, Leslie's conclusion is that the surface roughness increased the core radius. Monji and Wang (1989) studied the effect of different types of surface roughness on a laboratory tornado-like vortex. The roughness included cuboid blocks of 4X6X6 mm^3 spaced at 25 mm, and blocks of 9X6X6 mm^3 spaced at 25 mm, as well as a smooth surface for comparison. They concluded that increasing roughness enlarged the vortex core in cases with lower swirl ratios (S less than 0.3). On the contrary, with higher swirl ratios (S greater than 1.5), the changes to the vortex core was not significant. However, Diamond and Wilkins (1984) concluded that with a low aspect ratio, the core radius decreased with increasing surface roughness, which is not consistent with the results from the previous research mentioned above. Zhang and Sarkar (2008) studied

*Corresponding author, Assistant Professor
E-mail: yang@mst.edu

ISSN: 1226-6116 (Print), 1598-6225 (Online)

the effects of roughness on a laboratory-simulated tornado by using a 2-D PIV (Particle Image Velocimetry) technique. They found that the existence of surface roughness increased both the maximum radial and vertical velocities but decreased the maximum tangential velocity and core radius. The results on core radius are consistent with Diamond and Wilkins's results.

In addition, numerical simulations have also been conducted to determine the effects of surface roughness. Kuai *et al.* (2008) studied the effects of roughness using CFD (Computational Fluid Dynamics) simulations. Their results showed that increasing roughness greatly decreased the maximum tangential velocity but increased the core radius and swirl ratio of the vortex near the ground. Natarajan and Hangan (2009, 2011 and 2012) numerically studied the effects of mild roughness on tornado-like vortices with a wide range of swirl ratios from 0.1 to 2.0. Their results suggested that the surface roughness decreased the tangential velocity for all ranges of swirl ratios outside the core region, which is consistent with Kuai's results. However, in the core region, the existence of surface roughness increased the tangential velocity.

It is worth noting that the idealized surface roughness applied in previous research may not represent the real condition of the community of buildings. Through a comprehensive literature review, none of previous research has studied the influence of a community of buildings on tornadic wind fields by precisely modeling the surrounding structures in the computational domain. To bridge this research gap, in the present study, the community of buildings will be exactly modeled in the computational domain, as opposed to placing idealized blocks/rings in the wind field in previous research, and thus true characteristics of the tornadic wind field will be revealed. For comparison, besides the simulation of a translating tornado passing an urban area, the case in which only a single building is included in the tornadic wind field and the case in which the same community of buildings are present in the equivalent straight-line wind field are also simulated. The obtained results will contribute to tornado-resistant building design by providing more accurate wind effects.

The remaining of this paper is organized as follows. First, the three simulated cases, simulated tornadic and straight-line wind fields and CFD simulation setup are described; Second, the simulation results are presented to demonstrate the influence of a community of buildings on tornadic wind fields and to compare the worst condition between the community of buildings under tornadic wind fields and straight-line wind fields; Finally, conclusions are drawn and future work is discussed.

2. Simulated cases and simulation setup

2.1 Three simulated cases

Three cases are studied and compared. The first two cases are under tornadic wind field and the third case is under the equivalent straight-line wind field. The configuration for the community of buildings is to mimic a street block of buildings in Spencer, SD, which was hit by an F-4 tornado in 1998. In the first case, all buildings in the community are modeled in the computational domain (see Fig. 1(a)), designated as the "Community case under tornadic winds" hereafter, which is to simulate that a translating tornado passes an urban area. In the second case, only one building is included in the computational domain (see Fig. 1(b)), designated as the "Single-building case under tornadic winds", which is to simulate that a translating tornado passes a rural area. In the third case, all buildings in the community (same as in the first case) are modeled in the equivalent straight-line wind field (see Fig. 1(c)), designated as "Community case under straight-line winds", which is to simulate an urban area under straight-line winds. The wind direction is set to be perpendicular to the roof ridge. This is to be associated with an unfavorable case in tornadic fields, i.e., when the community center is located at the tornado core radius, the wind direction to the community is approximately perpendicular to the roof ridge.

In the Community cases under tornadic winds and straight-line winds, buildings included in the wind field are assumed to be identical and they are labeled from 1 to 18, as shown in Fig. 2(a). They are all gable-roofed houses with a floor plan of 35 m by 20 m, an eave height of 9 m and a roof height of 14 m, as shown in Fig. 2(b). In the Single-building case under tornadic winds, only one gable-roofed building with the same dimensions is included in the computational domain.

2.2 Simulated tornadic wind field

To simulate the tornadic wind field, a cylindrical computational domain with a velocity inlet and pressure outlet is applied. All other boundaries are defined as no-slip wall, as labelled in Figs. 1(a) and 1(b). The tangential velocity input, radial velocity input and vertical velocity input applied at the velocity inlet are based on the regression equations, Eqs. (1) through (5), from the radar-measured velocity data at the radius of 800 m of the Spencer, SD tornado of 30 May 1998 according to Pan and Xiao (2013). With the specific dimensions of pressure outlet (R=300 m) and velocity input (H=270 m), the tangential velocity profiles obtained from the simulation match those extracted from the radar-measured data very well. The pressure outlet was subject to the following settings: the static pressure relative to operating pressure is set as zero and the backflow direction specification method was set as Normal to Boundary.

$$\text{Tangential velocity: } V_t = 12.855(Z/20)^{0.2467} \tag{1}$$

$$\text{Radial velocity: } V_r = -32.851\left(\frac{Z}{20}\right)^{0.1346} \qquad Z \leq 20\ m \tag{2}$$

$$V_r = -59.92\left(\frac{Z}{20}\right)^{-0.2137} + 27.07 \qquad Z \leq 20\ m \tag{3}$$

$$\text{Vertical velocity: } V_v = 2(Z/800)(-32.851\left(\frac{Z}{20}\right)^{0.1346}) \qquad Z \leq 20\ m \tag{4}$$

$$V_v = 2(Z/800)(-59.92\left(\frac{Z}{20}\right)^{-0.2137} + 27.07) \qquad Z \leq 20\ m \tag{5}$$

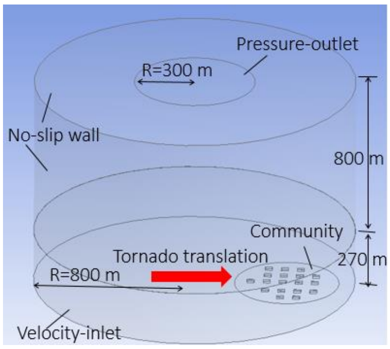

a) Community case under tornadic winds

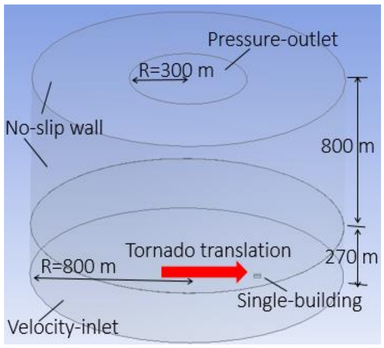

b) Single-building case under tornadic winds

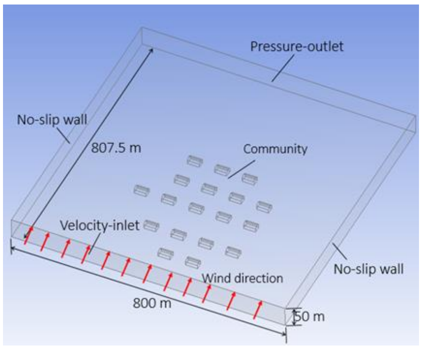

c) Community case under straight-line winds

Fig. 1 Computational domains for the three simulated cases

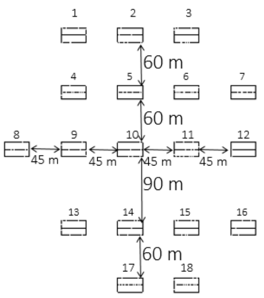

a) Numbering of the buildings in the community

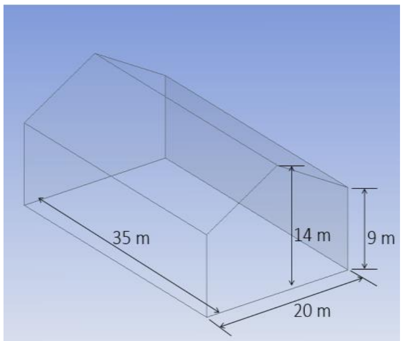

b) Dimensions of a building

Fig. 2 The simulated community with 18 identifical buildings

where Z is the height from the ground surface.

2.3 Simulation of tornado translation

In a real situation, the community of buildings is stationary and the tornado moves. To simulate the tornado translation, a relative motion is established, that is to say that the computational domain and the tornadic wind flow do not move and the buildings on the ground surface move at the same speed as tornado translation, but in the opposite direction. The translation speed of 15 m/s is applied here.

2.4 Simulation of the equivalent straight-line wind field

To simulate the equivalent straight-line wind field, a rectangular computational domain is applied, as shown in Fig. 1(c). At the velocity inlet, the velocity input with a power-law profile is applied. The velocity at the roof height is taken as the maximum resultant velocity at the roof height in the tornadic wind field at the core radius (the resultant velocity of tangential and radial velocities). It is 130.83 m/s. To simulate the urban/suburban areas, 0.14 is taken as the exponent of the power-law profile. Thus, the velocity profile at the velocity input is expressed as

$$V_s = 130.83(Z/H_r)^{0.14} \tag{6}$$

where V_s denotes the velocity at different heights; Z denotes the height above ground; and H_r denotes the reference height, which is the roof height (H_r= 14 m) here.

2.5 Setup of CFD simulation

The Large Eddy Simulation (LES) with dynamic Smagorinsky-Lilly subgrid model is adopted in this study.

The SIMPLEC (Semi-Implicit Method for Pressure Linked Equation-Consistent) method is used to solve N-S equations. The simulation is first run for 250 s to generate stationary tornadic winds, and then is run for 48 s to simulate the translation of tornadoes. During the 48 s, the Smoothing and Remeshing techniques are adopted as the dynamic meshing methods. For all of the three simulated cases, the mesh size is 1 m on the structure’s edges. The inflation technique is utilized in the region close to structural surface to avoid the adverse influence caused by the sudden change of the mesh size. The thickness of the first layer is 0.2 m, with a growth rate of 1.2 and a total number of layers of 15. In total, the number of the cells is approximately 1.8 million for the Single-building case under tornadic winds and 3.8 million for the Community case under tornadic winds. The time step of the simulation is 0.02 s.

It is noted that the current tornadic wind field is to simulate the Spencer, SD tornado of 30 May 1998 that was rated at F-4. To simulate tornadoes at other intensities (other EF scales), the magnitude of the velocities at the velocity inlet can be scaled accordingly.

3. Simulation results

For the Community cases under tornadic winds and straight-line winds, the tangential velocity and static pressure in the wind field are extracted when the tornado center reaches the community center and the tornado has a full access to all buildings in the community; for the Single-building case, the results are extracted when the core radius of the tornado reaches the building. Results are presented in four parts sequentially, the first is the one above the roof height, 14 m, and the second is the one below the roof height, as the influence of the presence of a community on tornadic wind fields is different in these two regions. The third one is the results at the elevation of 9 m when the most unfavorable conditions are observed. The last one is the comparison between the Community cases under tornadic winds and straight-line winds.

The ultimate goal of this research is to compare how different the wind pressure on the civil structure of interest (referred to “surface pressure”) is between the case when its surrounding structures are included in the computational domain and the case when its surrounding structures are not included. Considering that this surface pressure is directly related to the pressure in the wind field close to the structural surface and the pressure in the wind field is directly related to the velocity in the wind field, where appropriate, the comparisons are conducted in the sequence of Velocity in the Wind Field, Pressure in the Wind Field and Pressure on Structural Surface between cases.

3.1 Simulated tornadic wind field

The results for the tangential velocity distribution on the horizontal plane of 80 m are shown in Fig. 3. The color represents the magnitude of the tangential velocity and the arrows represent the direction of the resultant velocity of

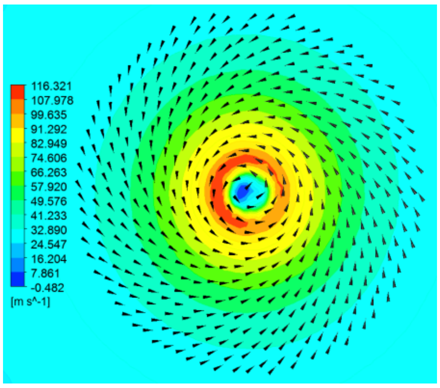

Fig. 3 Instantaneous Tangential velocity distribution on the horizontal plane at the elevation of 80 m

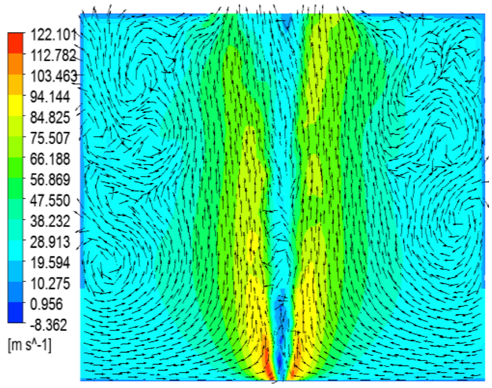

Fig. 4 Instantaneous Tangential velocity on a vertical plane through tornado center

tangential and radial components. Outside the core radius, the wind flow converges towards the tornado center, with increasing tangential velocity. A peak tangential velocity is found at the core radius, before decreasing along the radial distance from the core radius to the tornado center. In general, circular strips are formed, and the velocity in each strip is uniform, although the tangential velocity in the core is not as uniform, which may be due to the fact that the relatively lower rotational velocity cannot persist in the relatively higher turbulence in the core.

The Swirl ratio is calculated according to Eq. (7) from Liu and Ishihara (2015)

$$S_E = \frac{\Gamma_\infty}{2Qa} \tag{7}$$

where Γ_∞ is the free stream circulation at outer edge of convergence region, defined as $2\pi r_s h V_{rs}$, r_s is the core radius at a height of 80 m, h is the height of the velocity inlet, V_{rs} is the maximum tangential velocity at the core radius r_s at a height of 80 m, a is the aspect ratio, where a $= \frac{h}{r_o}$, where r_o is the pressure outlet radius, and Q is the total volume inflow rate. In this specific case the following values where used: r_s = 66 m, h = 270 m, V_{rs} = 116 m/s, r_o = 300 m, and Q = 2.05 x 107 m3/s. From this calculation the Swirl Ratio, S_E, was found to be 0.35. A swirl ratio of over 0.23 results in touch-down of the vortex according to Liu and Ishihara (2012). The current swirl ratio is well above this requirement.

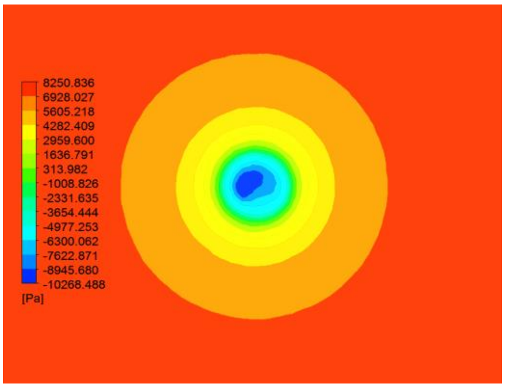

Fig. 5 Instantaneous Pressure distribution on the horizontal plane at the elevation of 80 m

The results for the tangential velocity distribution on a vertical plane through the tornado center are shown in Fig. 4. The color represents the magnitude of the tangential velocity and the arrows represent the direction of the resultant velocity of radial and vertical components. A downdraft is observed at the center and updrafts are observed on the surrounding areas. This suggests that the flow structure is double-celled, which is in agreement with the Spencer Tornado according to Kosiba and Wurman (2010). From the streamline on the vertical plane, as shown in Fig. 4, from the locations of vortex-streamline and the irregular streamline, vertical turbulence occurs on the two sides above 270 m and at tornado center at the lower elevations. From the streamline on the horizontal plane of H=80 m, in the outer region, stripes are regular, while stripes are irregular at around the core radius (as indicated by the red stripes) and inside the core. By investigating the streamline on other elevations, a similar phenomenon is observed. Thus, by combining the observations from both the horizontal planes and vertical planes, the turbulence field is located in the tornado core at lower elevations, while it is located outside the tornado core at higher elevations.

The results for the pressure contour on the horizontal plane at the elevation of 80 m are shown in Fig. 5. Regular circular strips are observed. The pressure gradually decreases along the radius from the outer edge to tornado center, and this pressure gradient helps to show why the air flows inwards while rotating outside the core.

3.2 Tangential velocity at heights above 14 m

The results for the tangential velocity contours on four horizontal planes associated with four different heights (14.5 m, 16 m, 20 m and 30 m) for the Community case under tornadic winds are shown in Fig. 6. Fig. 7 is for the Single-building case under tornadic winds. In each figure, the color represents the magnitude range of the tangential velocity and the arrows represent the projection of the resultant velocity (the resultant velocity of tangential and radial components) on the horizontal plane (indicating the wind direction). It is noted that no building blockage is present above 14 m.

By comparing the figures at each elevation between the two cases, it is observed that regular circular strips are well maintained in the Single-building case under tornadic winds (see all subfigures in Fig. 7), while the regular circular strips are destroyed in the Community case under tornadic winds due to the residual effects induced by the presence of a community of buildings (see Figs. 6(a) and 6(b)). In the Community case under tornadic winds, this effect gradually decreases as the elevation increases, and regular circular strips are gradually recovered along the height (see Figs. 6(c) and 6(d)). Accordingly, it is difficult to determine the core radius in the Community case under tornadic winds at lower elevations, while it is easy to determine the core radius from the regular circular strips at a height of 30 m or above. At the height of 30 m, the core radius of this tornado is 47 m.

In both cases, above 14 m, the peak tangential velocity (red color) occurs at the projection location(s) of building(s), this is due to the residual effect of the building blockage below 14 m. In the Community case under tornadic winds, the maximum tangential velocity is 147 m/s, which is lower than that in the Single-building case under tornadic winds (157 m/s). In addition, in both cases, the maximum wind velocity of the main flow (except the flow indicated by red color) can be represented by the yellow color at the heights below 20 m (see Subfigures (a), (b) and (c) in Figs. 6 and 7) and by the orange color at the height of 30 m. By comparing the scale bars in Figs. 6 and 7 at each height, the magnitude of the maximum velocity of the main flow in the Community case under tornadic winds is lower than that in the Single-building case under tornadic winds. All this is due to the fact that the surface friction in the Community case is higher compared to the Single-building case. The difference in surface friction between the two cases becomes smaller and smaller as the elevation increases, as indicated by the observation that the difference in the magnitude of tangential velocity between the two cases becomes smaller and smaller with increasing elevation (see Subfigures (a), (b) and (c) in Figs. 6 and 7) and becomes similar at the height of 30 m (see Figs. 6(d) and 7(d)).

A negative tangential velocity is observed in both cases. A negative tangential velocity means that the air flows in the clockwise direction (a counter-clockwise tornado occurring in North Hemisphere is simulated here). It is caused by the wake effect of building blockage at lower elevations (below 14 m), the wake effect at lower elevations extends to higher elevations (above 14 m) to become a residual effect. In the Single-building case under tornadic winds, the wake effect and residual effect are weaker so that the negative tangential velocity almost disappears at the height of 20 m. By contrast, in the Community case under tornadic winds, the residual effect is so strong that the negative tangential velocity is still observable at higher elevations (30 m).

3.3 Pressure distribution at heights above 14 m

Pressure in the wind field is presented in the form of pressure coefficients. In this study, the pressure coefficient

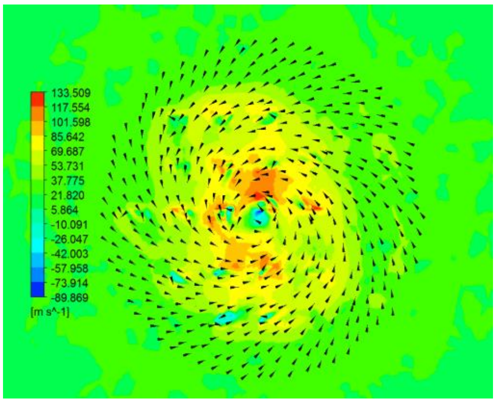

a) At the elevation of 14.5 m

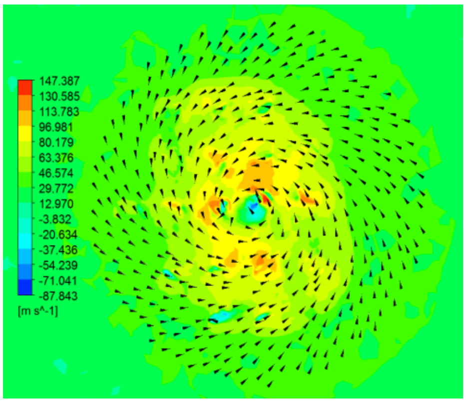

b) At the elevation of 16 m

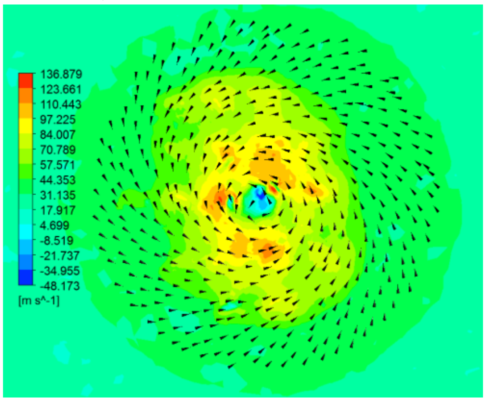

c) At the elevation of 20 m

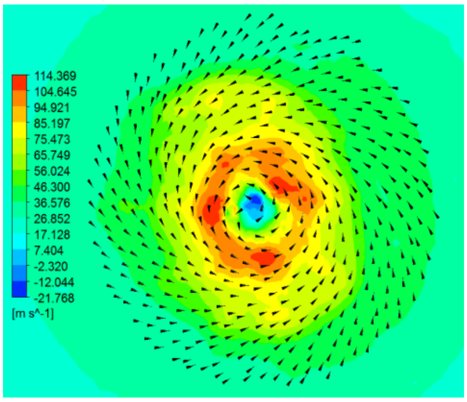

d) At the elevation of 30 m

Fig. 6 Tangential velocity distribution on the horizontal plane for the Community case under tornadic winds above 14 m

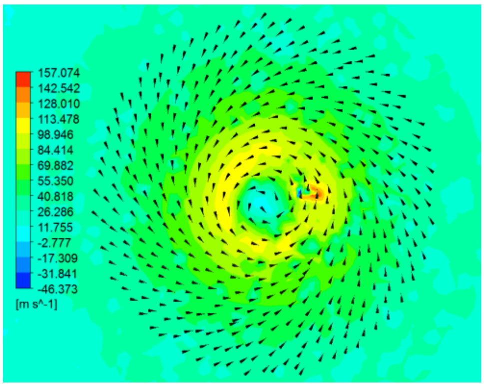

a) At the elevation of 14.5 m

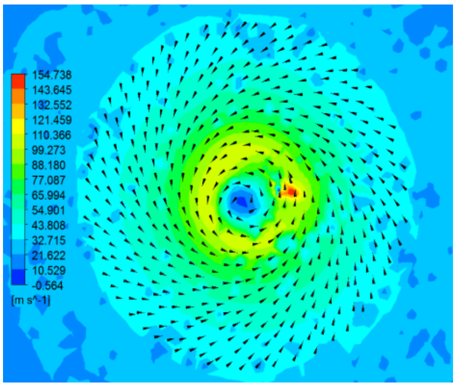

b) At the elevation of 16 m

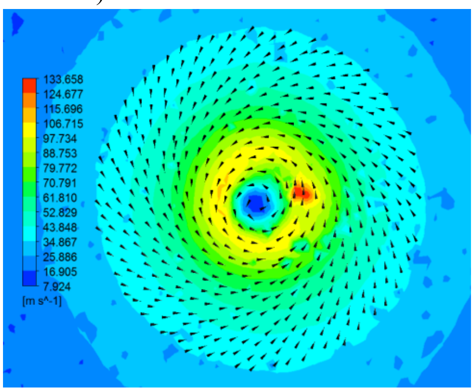

c) At the elevation of 20 m

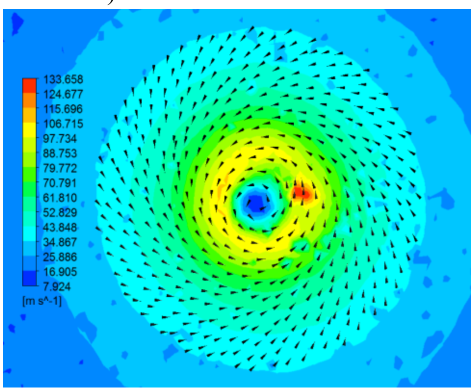

d) At the elevation of 30 m

Fig. 7 Tangential velocity distribution on the horizontal plane for the Single-building case under tornadic winds above 14 m presented is extracted based on Eq. (8)

$$C_p = \frac{P - P_r}{\frac{1}{2}\rho_r V_r^2} \tag{8}$$

where $P - P_r$ denotes the relative static pressure at the point where the pressure coefficient is evaluated. In all of the three cases, $\mathrm{P_r}$, $\mathrm{V_r}$, and $\mathrm{\rho_r}$ denote the reference pressure, reference wind velocity and air density, respectively, which are $P_r = 101325$ Pa, $V_r = 98.7$ m/s and $\rho_r = 1.225$ kg/m^3 in this study.

The pattern of regular circular strips is observed in the pressure distribution in the wind field of the Single-building case, as shown in Fig 9. This is consistent with the pattern of the tangential velocity distribution for the Single-building case (see Fig. 7). However, for the Community case under tornadic winds, the pattern of regular circular strips is destroyed at lower elevations due to the presence of a number of buildings (see Figs. 8(a) and 8(b)), and the regular circular pattern is recovered as the elevation increases, which is consistent with the observation in tangential velocity.

The maximum positive pressure coefficient is observed in the outer region for both cases at any heights above 14 m, as shown in Figs. 8 and 9, because the tangential velocity in the outer region is very low which lead to larger pressure, according to Bernoulli Equation. The maximum positive pressure coefficient is nearly the same through all heights for each case. The maximum positive pressure coefficient in the Community case under tornadic winds is always higher than that in the Single building case under tornadic winds, due to the fact that the tangential velocity is lower in the outer region for the Community case than that in the Single building case, leading to a higher pressure at the outer region. —It is noted that the above analysis based on Bernoulli Equation discusses the relationship between pressure and tangential velocity, although Bernoulli Equation theoretically relates pressure to resultant velocity. The above analysis is valid due to the following two reasons. First, tangential velocity is the primary component of the resultant velocity in most regions; Second, the tangential velocity has been presented above and thus this quantity can be qualitatively related to the pressure. It is worth noting that the above analysis is qualitative, as Bernoulli Equation is not strictly applicable to rotational flow.

In both cases, at the elevations of 14.5 m, 16 m and 20 m, the maximum negative pressure coefficient is observed around the projection locations of the building(s), which is caused by the wake effect (small vortex) and residual effect induced by the presence of the building(s), conversely, at the elevation of 30 m, the maximum negative pressure is observed at the tornado center, which is caused by the atmospheric pressure drop at the tornado center. In the Single-building case under tornadic winds, the maximum negative pressure coefficient decreases with the increase in elevation. In the Community case under tornadic winds, for most of the elevations, the maximum negative pressure is greater than that in the Single-building case under tornadic winds. The magnitude difference between these two cases becomes smaller at the height of 30 m. This is because the residual effect caused by the presence of the building(s) becomes smaller at 30 m and the atmospheric pressure drop at the tornado center dominates the negative pressure at 30 m.

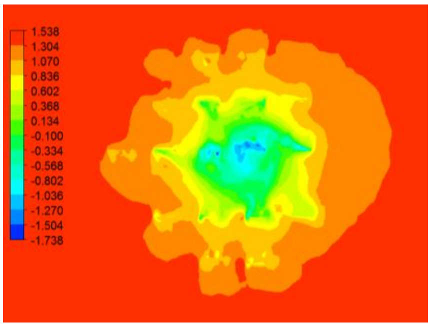

a) At the elevation of 14.5 m

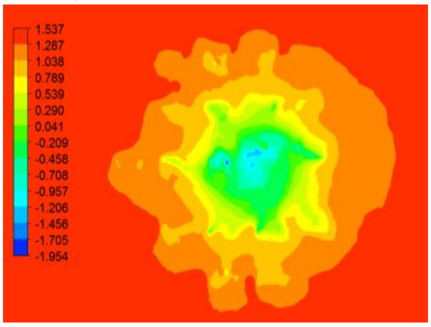

b) At the elevation of 16 m

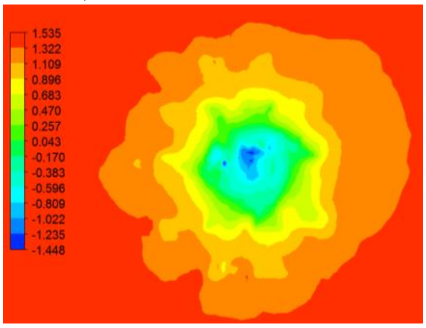

c) At the elevation of 20 m

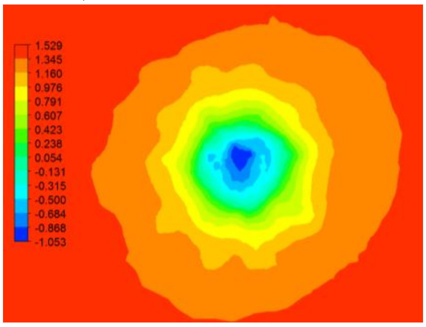

d) At the elevation of 30 m

Fig. 8 Pressure coefficient contour on the horizontal plane for the Community case under tornadic winds above 14 m

3.4 Effects of building populating density on surface friction

To demonstrate the influence of building populating

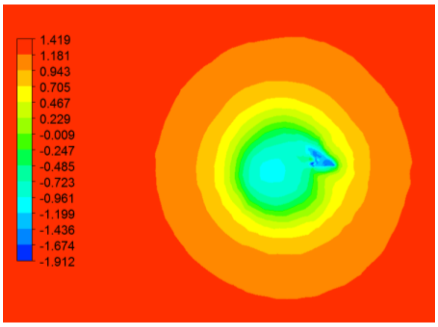

a) At the elevation of 14.5 m

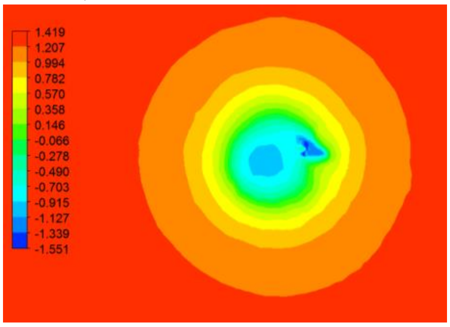

b) At the elevation of 16 m

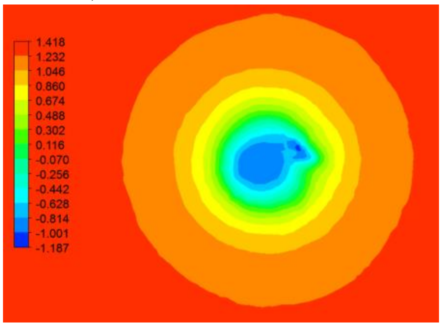

c) At the elevation of 20 m

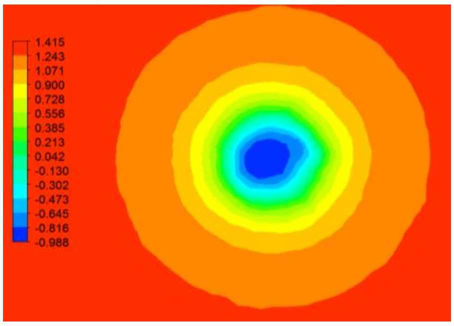

d) At the elevation of 30 m

Fig. 9 Pressure coefficient contour on the horizontal plane for the Single-building case under tornadic winds above 14 m

density on surface friction, the tangential velocity profile along a vertical line is extracted at the same location for both cases (see the black point in Figs. 10 and 11) and they are presented in Figs. 12 and 13, respectively. The black points are chosen to be far away from the building(s) in order to better capture the wind velocity of the overall wind flow. Near ground (lower than 30 m), at the same height, the tangential velocity in the Community case under tornadic winds is much lower than that in the Single-building case under tornadic winds. This further verifies that the surface friction in the Community case under tornadic winds is much higher than that in the Single-building case under tornadic winds.

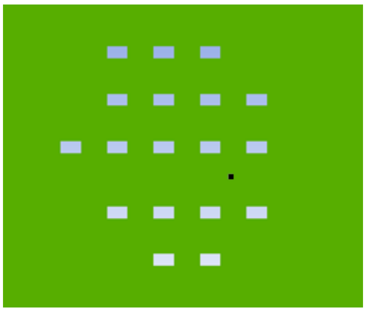

Fig. 10 Location at which the vertical line of tangential velocity is extracted in the Community case under tornadic winds

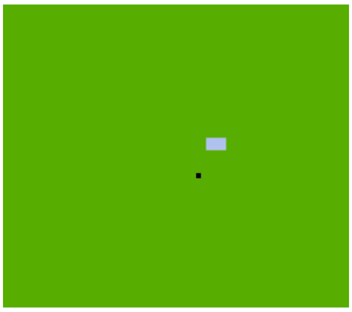

Fig. 11 Location at which the vertical line of tangential velocity is extracted in the Single-building case under tornadic winds

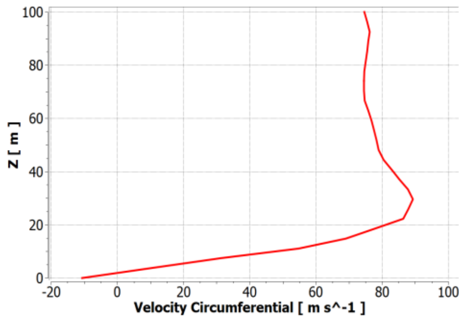

Fig. 12 Tangential velocity profile along a vertical line for the Community case under tornadic winds

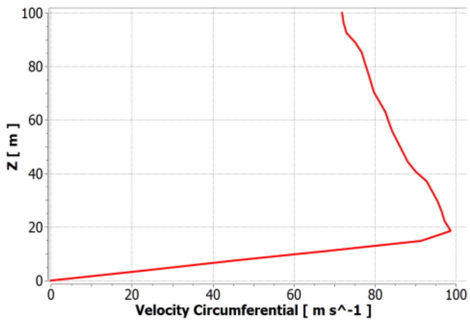

Fig. 13 Tangential velocity profile along a vertical line for the Single-building case under tornadic winds

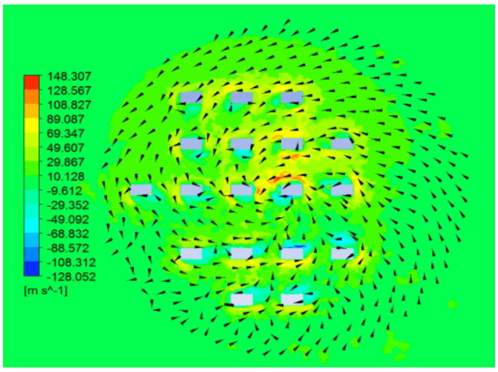

a) At the elevation of 3 m

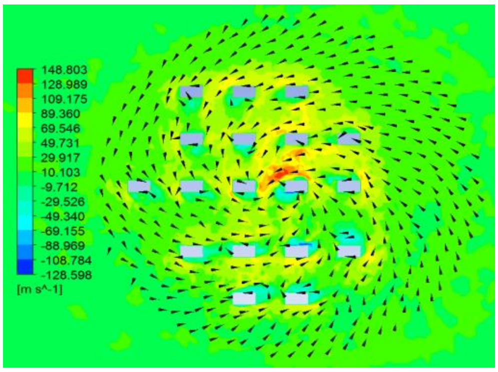

b) At the elevation of 5 m

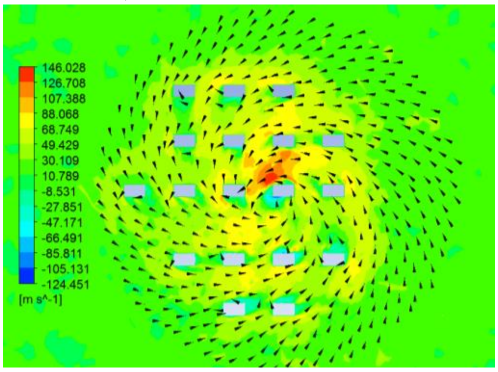

c) At the elevation of 9 m

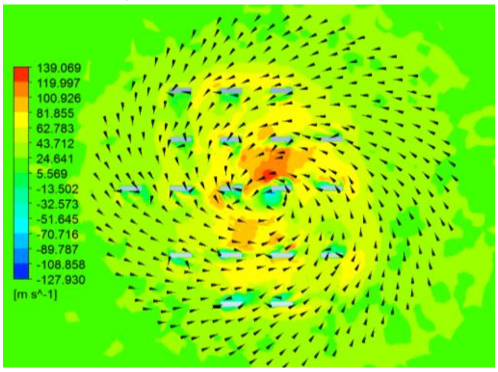

d) At the elevation of 12 m

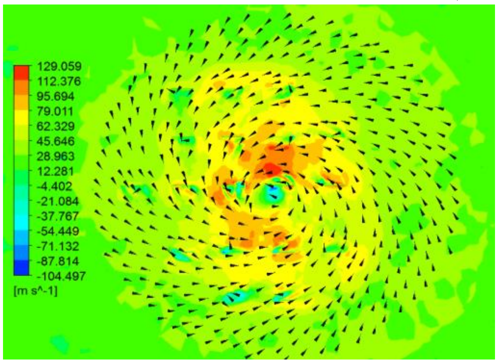

e) At the elevation of 14 m

Fig. 14 Tangential velocity distribution on the horizontal plane for the Community case under tornadic winds below 14 m

3.5 Tangential velocity at heights below 14 m

The results for the tangential velocity contours on five horizontal planes associated with the heights that are lower than or equal to the roof height, which are 3 m, 5 m, 9 m, 12 m and 14 m, are shown in Figs. 14 and 15. From Fig. 15, for the Single-building case under tornadic winds, except the region around the building, the pattern of regular circular strips is well maintained, and the core radius can still be easily determined, which is 75 m at the height of 14 m. However, for the Community case under tornadic winds (see Fig. 14), the pattern of regular circular strips is completely destroyed due to the presence of a number of buildings, while the spiral pattern is extended towards the tornado center, although the spiral pattern at the tornado center is outward. Obviously, for the Community case under tornadic winds, the original definition of core radius (the radius with the maximum tangential velocity) may not be applicable here. By comparing the figures associated with different elevations for the Community case under tornadic winds, this effect tends to decrease with the increase in elevation.

From each figure, the maximum tangential velocity is always observed around the building(s) for both cases. This can be explained by the building blockage resulting in increased velocity around the buildings. The higher maximum tangential velocity below 14 m (148 m/s shown in Fig. 14(b)) occurs in the Community case under tornadic winds between buildings inside the community. This is due to the following potential reasons: 1) when the wind flow passes two sequential buildings, due to the short distance between the two buildings, the accelerated velocity due to the blockage of the first building is further accelerated when the wind flow passes the next building; or 2) a canyon street effect induced by the two buildings parallel to the wind direction may increase the speed of the wind passing between the two buildings.

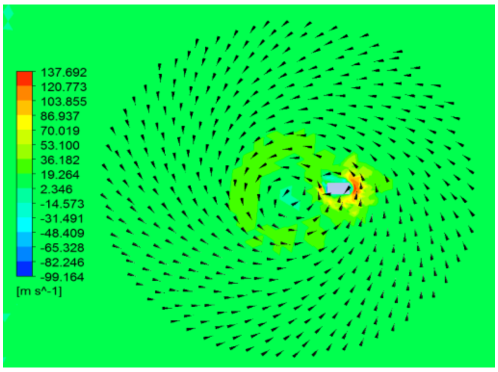

a) At the elevation of 3 m

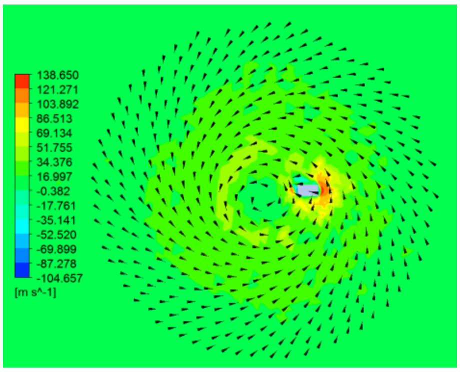

b) At the elevation of 5 m

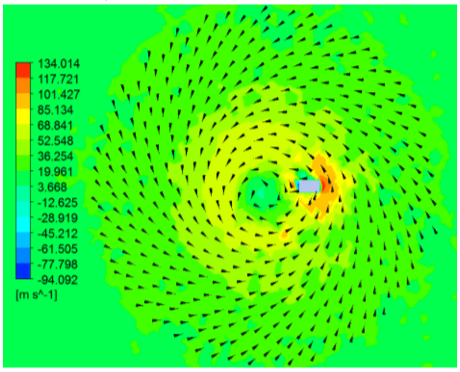

c) At the elevation of 9 m

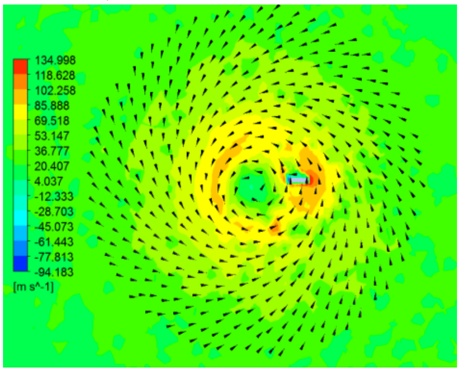

d) At the elevation of 12 m

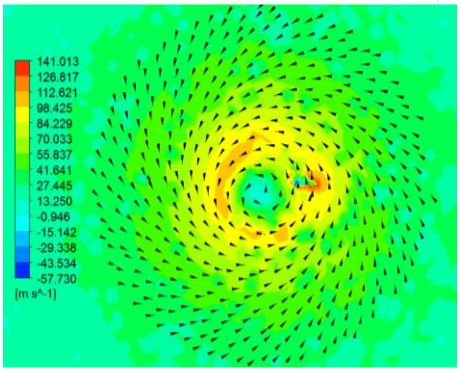

e) At the elevation of 14 m

Fig. 15 Tangential velocity distribution on the horizontal plane for the Single-building case under tornadic winds below 14 m

3.6 Pressure distribution at heights below 14 m

For the Single-building case under tornadic winds, below 14 m, the static pressure can still be considered uniform, with regular circular strips, except the region around the building. That is, the wind field is not affected much by a single building. For the Community case under tornadic winds, the regular circular strip pattern is completely destroyed due to the presence of multiple buildings.

From Figs. 16 and 17, below 14 m, the maximum negative pressure is always observed around the buildings for both of these two case, which is caused by the vortices formed on the two sides or the wake of the building(s) (the wake effect). The maximum positive pressure for the Community case under tornadic winds is observed on the windward side of a building, while it is observed in the outer region for the Single-building case under tornadic winds. The greater maximum positive pressure is obtained in the Community case under tornadic winds, which is 1.938, as shown in Fig. 16(b). The greater maximum negative pressure is obtained in the Single-building case, which is -2.256, as shown in Fig. 17(e). It is worth noting that these results are only for the case when the community center moves to the center of computational domain, which is not the worst scenario for the tornado case, as shall be shown in Section 3.7.

3.7 Comparison on maximum pressure values at 9 m between the two tornadic cases

For civil structures in a community environment, the wall height, the elevation of 9 m, is considered to be a primary focus for design loading considerations Figs. 18 - 23 present the maximum tangential velocity and wind

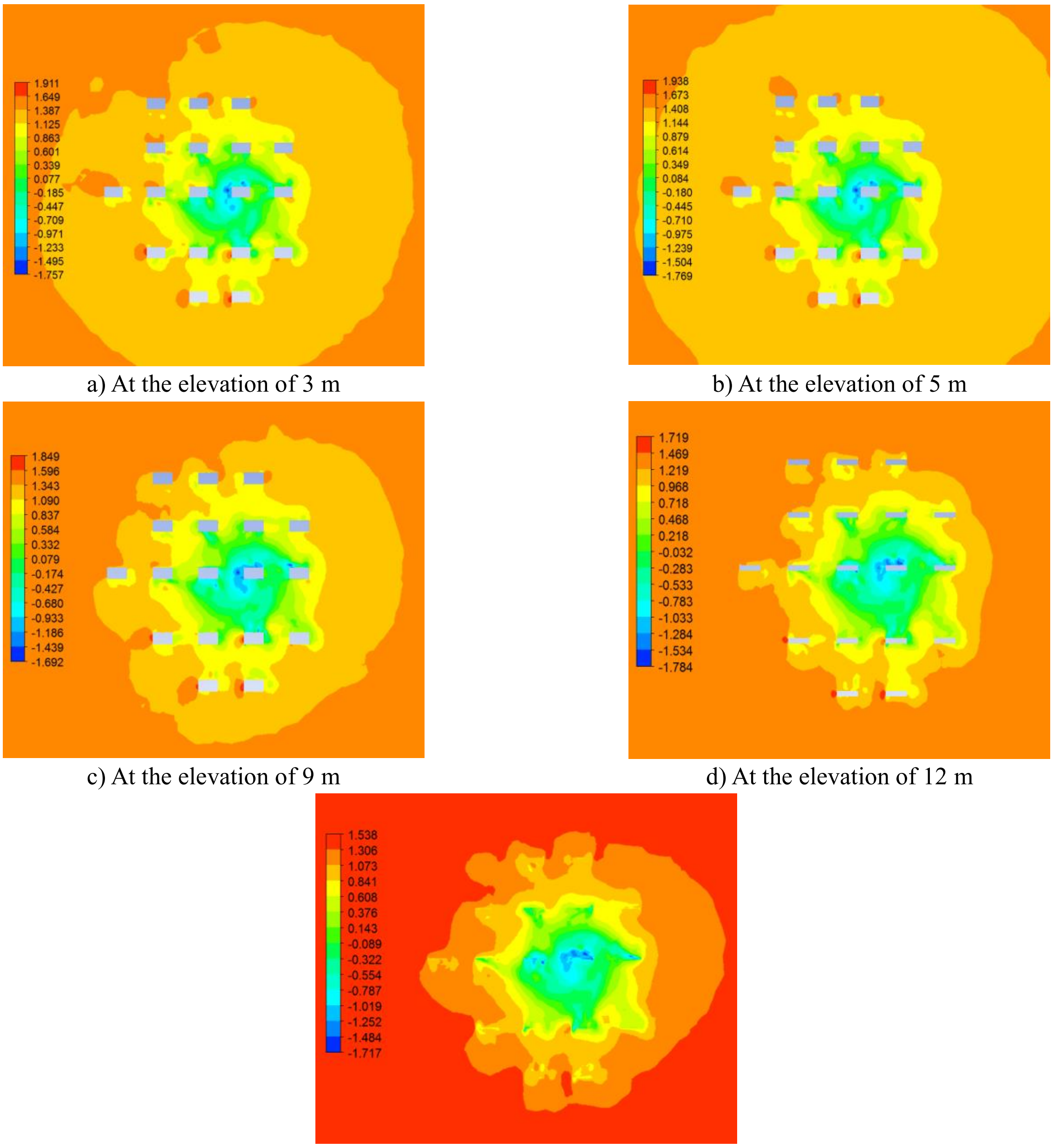

a) At the elevation of 3 m

b) At the elevation of 5 m

c) At the elevation of 9 m

d) At the elevation of 12 m

e) At the elevation of 14 m

Fig. 16 Pressure coefficient contour on the horizontal plane for the Community case under tornadic winds below 14 m

pressure coefficient on the horizontal plane for the Community case under tornadic winds and the Single-building case under tornadic winds at 9 m. This is to look for the most unfavorable conditions in each tornadic case. It is noted that the location(s) of building(s) relative to tornado center may vary among all these figures. By comparing the maximum magnitude of these results, the greater maximum tangential velocity and pressure coefficient are observed in the Community case under tornadic winds, which means that the more unfavorable conditions occur in the Community case under tornadic winds.

For the community case under tornadic winds, the maximum tangential velocity is observed when the community center is 115 m away from the center of computational domain, as shown in Fig. 18. The maximum positive and negative pressure is observed when the community center is 42.5 m and 102.5 m away from the center of computational domain, as shown in Figs. 20 and 22 respectively. For the single-building case, the maximum tangential velocity is observed when this building is 60 m away from tornado center, as shown in Fig. 19 the maximum positive and negative pressure is observed when this building is 307.5 m and 67.5 m away from the tornado center, respectively, as shown in Figs. 21 and 23.

3.8 Comparison between the community case under tornadic winds and the community case under straight-line winds at 9 m

The results for the pressure coefficient on the horizontal plane at 9 m in the Community case under straight-line

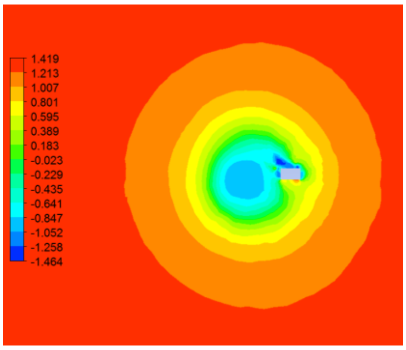

a) At the elevation of 3 m

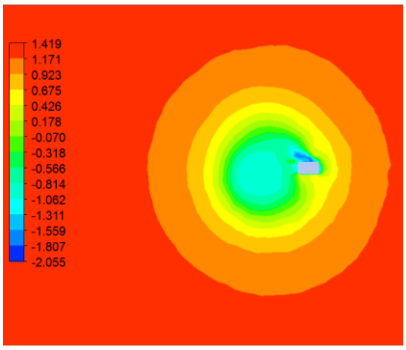

b) At the elevation of 5 m

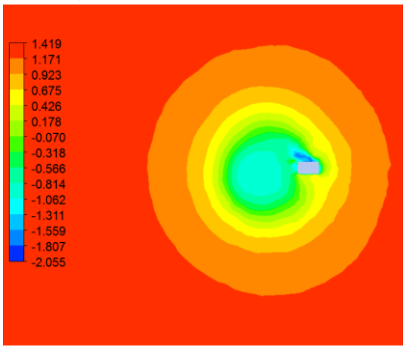

c) At the elevation of 9 m

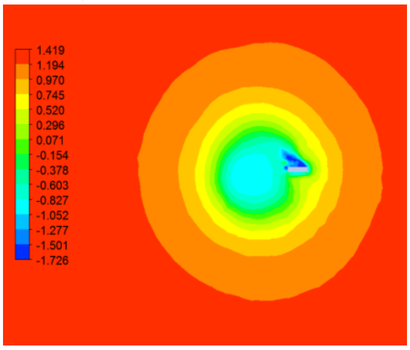

d) At the elevation of 12 m

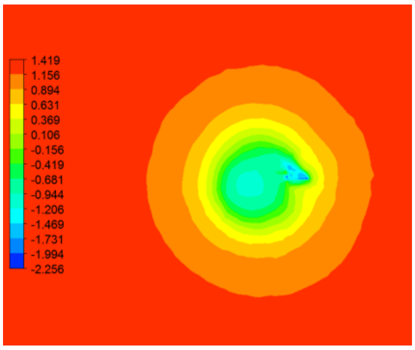

e) At the elevation of 14 m

Fig. 17 Pressure coefficient contour on the horizontal plane for the Single-building case under tornadic winds below 14 m

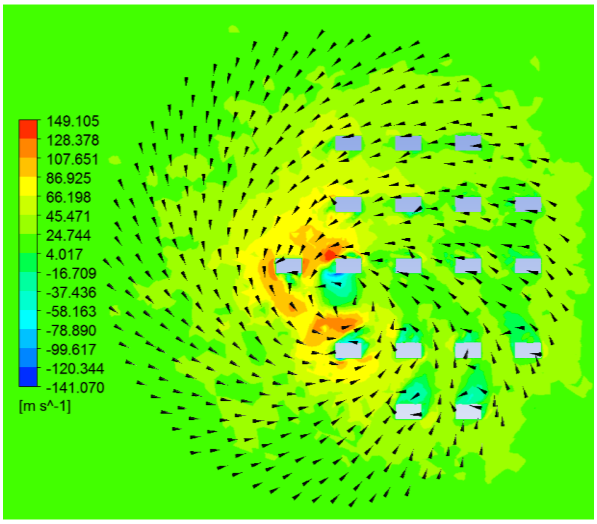

Fig. 18 Tangential velocity distribution on the horizontal plane at the elevation of 9 m for the Community case under tornadic winds when the maximum tangential velocity is observed

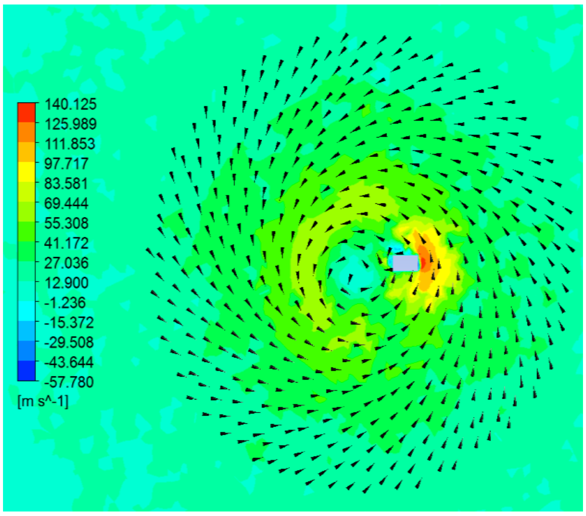

Fig. 19 Tangential velocity distribution on the horizontal plane at the elevation of 9 m for the Single-building case under tornadic winds when the maximum tangential velocity is observed

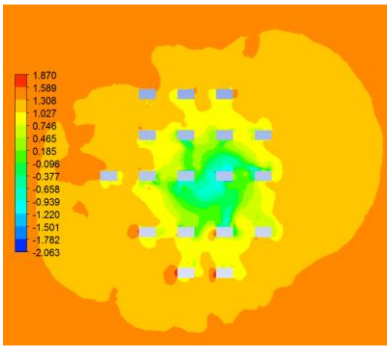

Fig. 20 Pressure coefficient contour on the horizontal plane at the elevation of 9 m for the Community case under tornadic winds when the maximum positive pressure is observed

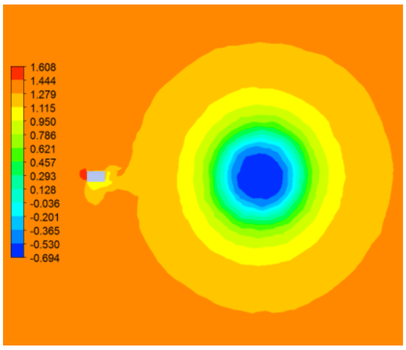

Fig. 21 Pressure coefficient contour on the horizontal plane at the elevation of 9 m for the Single-building case under tornadic winds when the maximum positive pressure is observed

winds are shown in Fig. 24. By comparing Figs. 20, 22 and 24, at the wall height (9 m), both of the maximum positive pressure and maximum negative pressure coefficient in the tornadic wind field (1.87 and -4.05, as shown in Figs. 20 and 22, respectively) are greater than those in the straight-line wind field (1.24 and -1.54, as shown in Fig. 24).

The results for the pressure coefficient on the structural surface of Building No. 10 for the Community case under tornadic winds, when the maximum positive and negative surface pressure is observed, are shown in Figs. 25 and 26. Fig. 27 presents the pressure on the structural surface of Building No. 10 for the Community case under straight-line winds. By comparing these figures, the results also demonstrate that the greater maximum positive and negative pressure coefficient, 1.66 and -2.87, are obtained in the tornadic winds field when the community center is 215 m and 17.5 m away from the center of the computational domain, as shown in Figs. 25 and 26, which are respectively 1.54 and 1.98 times higher than the maximum positive and negative pressure in Fig. 27. That means Building No. 10 experiences more unfavorable conditions in the tornadic wind field. In the literature, Yousef et al (2018) compared the wind effects on a prism induced by tornadic winds and equivalent straight-line winds. They found that the maximum negative pressure on structural surface was 1.75 times larger in the tornadic case. This presents a reasonable comparison to the surface pressure obtained on Building No. 10 (1.98 times larger in the tornadic wind field case than in the equivalent straight-line wind field case).

The results for the velocity distribution on the horizontal plane at the elevation of 9 m for the Community case under straight-line winds are shown in Fig. 28. By comparing the Figs. 18 and 28, it shows that the maximum positive velocity in the straight-line winds field (160 m/s) is greater than that in the tornadic winds (149 m/s). However, because the positions where the maximum velocity happened are not in front of the windward wall of Building No. 10, it would not lead to greater positive pressure on the structure surface in the straight-line wind case.

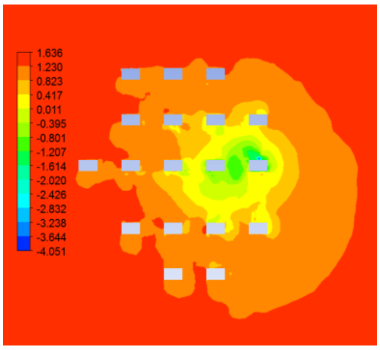

Fig. 22 Pressure coefficient contour on the horizontal plane at the elevation of 9 m for the Community case under tornadic winds when the maximum negative pressure is observed

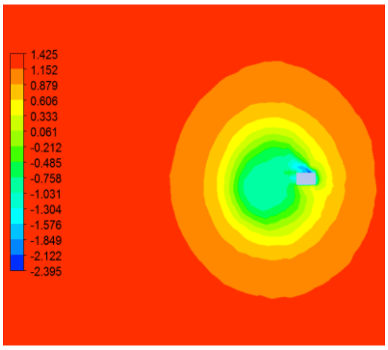

Fig. 23 Pressure coefficient contour on the horizontal plane at the elevation of 9 m for the Single-building case under tornadic winds when the maximum negative pressure is observed

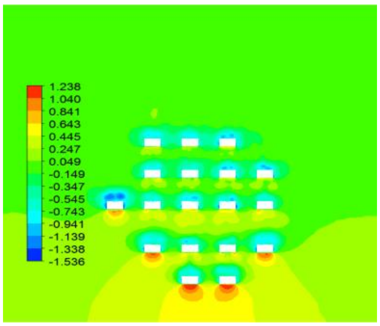

Fig. 24 Pressure coefficient contour on the horizontal plane at the elevation of 9 m for the Community case under straight-line winds

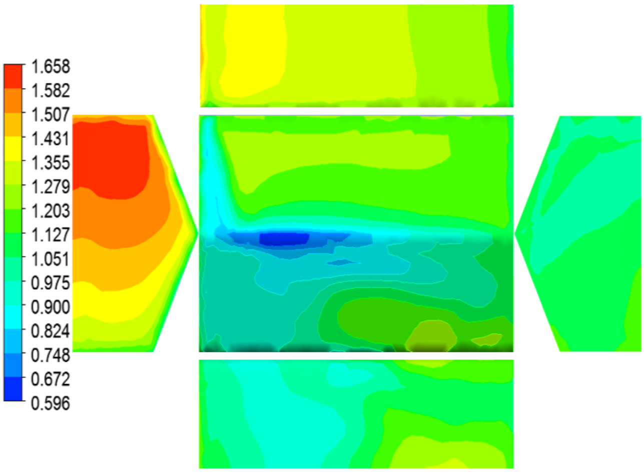

Fig. 25 Pressure coefficient on the structural surfaces of Building No. 10 for the Community case under tornadic winds when the maximum positive surface pressure is observed

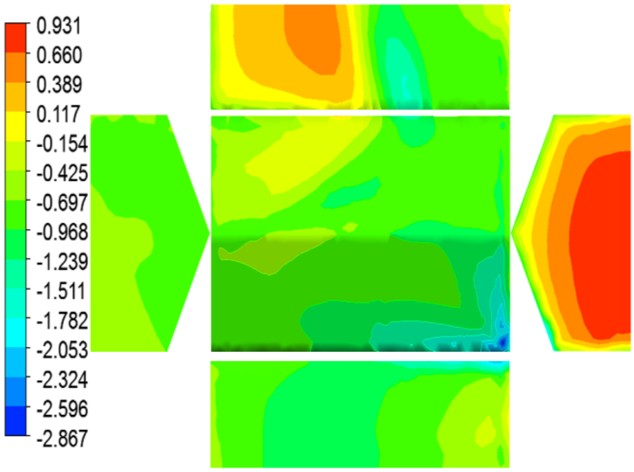

Fig. 26 Pressure coefficient on the structural surface of Building No. 10 for the Community case under tornadic winds when the maximum negative surface pressure is observed

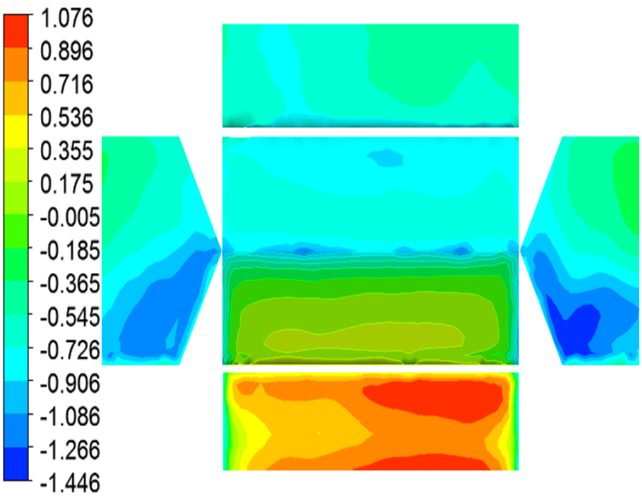

Fig. 27 Pressure coefficient on structural surface of Building No. 10 for the Community case under straight-line winds

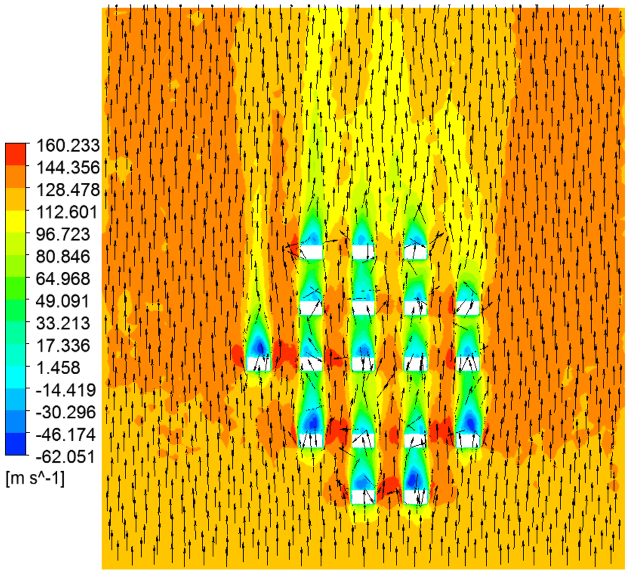

Fig. 28 Velocity distribution on the horizontal plane at the elevation of 9 m for the Community case under straight-line winds

4. Conclusions

In this study, the influence of a community of buildings on tornadic wind fields is systematically investigated by modeling all buildings in the community into the wind field. For comparison, the case in which only a single building is included in the tornadic wind field and the case where a community of buildings are included in the equivalent straight-line wind field are also simulated. The following conclusions can be drawn:

- At the elevations above the roof height (14 m), the regular circular strip pattern in the distribution of tangential velocity on horizontal planes are completely destroyed in the Community case under tornadic winds, due to the residual effects induced by the presence of a community of buildings. The residual effects become weaker as the elevation increases, and the strip pattern is recovered at the elevation of 30 m. By contrast, in the Single-building case under tornadic winds, the regular circular pattern remains very well except at the projection location of the single building. In the Community case under tornadic winds, the maximum tangential velocity (147 m/s) is lower than that in the Single-building case under tornadic winds (157 m/s), because of the greater surface friction caused by the community of buildings.
- At the elevations below the roof height, the regular circular strip pattern in the distribution of tangential velocity is also destroyed. At all elevations below the roof height, greater maximum tangential velocity and maximum positive pressure are observed in the Community case under tornadic winds potentially due to the obstruction of a number of buildings and the canyon street effect.
- To be specific, at the elevation of 9 m, the maximum tangential velocity (149 m/s), positive pressure coefficient (1.87), and negative pressure coefficient (-

4.05) obtained in the Community case under tornadic winds are greater than those in the Single-building case under tornadic winds, which are 140 m/s, 1.61 and -2.40, respectively. By comparing the results, the more unfavorable scenario is found in the Community case under tornadic winds, instead of in the Single-building case under tornadic winds.

• By comparing the Community case under tornadic winds and equivalent straight-line winds, at the elevation of 9 m, the maximum positive pressure coefficient (1.87) and negative pressure coefficient (-4.05) obtained in the Community case under tornadic winds are 1.51 times and 2.63 times greater than those under in the equivalent straight-line winds, which are 1.24 and -1.54, respectively. This suggests that more unfavorable scenario is obtained in the tornadic wind field, instead of in the equivalent straight-line winds.

• For the wind pressure on structural surface of No. 10 building in the community, the maximum positive pressure coefficient (1.66) and negative pressure coefficient (-2.87) obtained in the Community case under tornadic winds are 1.54 times and 1.98 times greater than those in the equivalent straight-line winds, which are 1.08, and -1.45, respectively. This demonstrates that Building No. 10 experiences more unfavorable conditions in the tornadic wind field.

The obtained research results suggest that tornadic wind loading will be underestimated if the surrounding structures of the civil structure of interest are not included in the computational domain. Therefore, to properly quantify the tornadic wind loading, both the civil structure of interest and its surrounding structures should be included in the computational domain. Currently, Chapter 26 in the commentary of ASCE 7-16 provides the “Extended Method” and “Simplified Method” for tornado-resistant design. The Extend Method is to modify the coefficients in the pressure calculation equation that was originally developed for straight-line winds. The Extend Method specifies that the design terrain must be “C” or “D”, no matter whether the original design terrain is “B”, “C” or “D”, which is used to determine the value of the Kz coefficient. As far as the present authors are concerned, this specification ignores the influence of surrounding buildings on the tornadic wind fields and thus cannot properly determine the tornado-induced pressure. The developed approach in this study can be used to properly modify the Kz value.

Since the simulated community of buildings represent a general residential community pattern, the obtained results can be used to modify the Kz value for the case where a tornado with a relatively high intensity strikes a regular residential community. The currently obtained results may depend on the particular pattern and layout of the community. In the future, systematical simulation will be conducted to investigate how the current trend is changed when the relative size between the tornado core radius and community size changes and when the tornado intensity changes.

References

Blocken, B., Stathopoulos, T. and van Beeck, J.P.A.J. (2016), “Pedestrian-level wind conditions around buildings: Review of wind-tunnel and CFD techniques and their accuracy for wind comfort assessment”, *Build. Environ*., **100**, 50-81. https://doi.org/10.1016/j.buildenv.2016.02.004.

Chang, C.H. and Meroney, R.N. (2003), “The effect of surroundings with different separation distances on surface pressures on low-rise buildings”, *J. Wind Eng. Ind. Aerod*., **91**(8), 1039-1050. https://doi.org/10.1016/S0167-6105(03)00051-5.

Dessens Jr, J. (1972), “Influence of ground roughness on tornadoes: A laboratory simulation”, *J. Appl. Meteorol*., **11**(1), 72-75.

Diamond, C.J., and Wilkins, E.M. (1984), “Translation effects on simulated tornadoes”, *J. Atmos. Sci*., **41**(17), 2574-2580.

Elshaer, A., Aboshosha, H., Bitsuamlak, G., El Damatty, A. and Dagnew, A. (2016), “LES evaluation of wind-induced responses for an isolated and a surrounded tall building”, *Eng. Struct*., **115**, 179-195. https://doi.org/10.1016/j.engstruct.2016.02.026.

Khanduri, A.C., Stathopoulos, T. and Bédard, C. (1998), “Wind-induced interference effects on buildings - a review of the state-of-the-art”, *Eng. Struct*., **20**(7), 617-630. https://doi.org/10.1016/S0141-0296(97)00066-7.

Kosiba, K. and Wurman, J. (2010). “The three-dimensional axisymmetric wind field structure of the Spencer, South Dakota, 1998 Tornado”, *J. Atmos. Sci*., **67**, 3074-3083.

Kuai, L., Haan Jr, F.L., Gallus Jr, W.A. and Sarkar, P.P. (2008), “CFD simulations of the flow field of a laboratory-simulated tornado for parameter sensitivity studies and comparison with field measurements”, *Wind Struct*., **11**(2), 75-96.

Lam, K.M., Leung, M.Y.H. and Zhao, J.G. (2008), “Interference effects on wind loading of a row of closely spaced tall buildings”, *J. Wind Eng. Ind. Aerod*., **96**(5), 562-583. https://doi.org/10.1016/j.jweia.2008.01.010.

Lam, K.M., Zhao, J.G. and Leung, M.Y.H. (2011), “Wind-induced loading and dynamic responses of a row of tall buildings under strong interference”, *J. Wind Eng. Ind.Aerod*., **99**(5), 573-583. https://doi.org/10.1016/j.jweia.2011.02.006.

Leslie, F.W. (1977), “Surface roughness effects on suction vortex formation: A laboratory simulation”, *J. Atmos. Sci.*, **34**(7), 1022-1027.

Liu, Z. and Ishihara, T. (2012), “Effects of the swirl ratio on turbulent flow fields of tornado-like vortices by using LES turbulent model”, *The Seventh International Colloquium on Bluff Body Aerodynamics and Applications (BBAA7)*, Shanghai, China, September.

Liu, Z. and Ishihara, T. (2015). “Numerical study of turbulent flow fields and the similarity of tornado vortices using large-eddy simulations”, *J. Wind Eng. Ind.Aerod*., **145**, 42-60. https://doi.org/10.1016/j.jweia.2015.05.008.

Monji, N. and Wang, Y.K. (1989), “A laboratory investigation of characteristics of tornado-like vortices over various rough surfaces”, *J. Meteo. Res*., **3**(4), 506-515.

Natarajan, D. (2011), “Numerical simulation of tornado-like vortices”, Ph.D. Dissertation, The University of Western Ontario, Ontario, Canada.

Natarajan, D. and Hangan, H. (2009), “Numerical study on the effects of surface roughness on tornado-like flows”, *In 11th Americas Conference on Wind Engineering*.

Natarajan, D. and Hangan, H. (2012), “Large eddy simulations of translation and surface roughness effects on tornado-like vortices”, *J. Wind Eng. Ind.Aerod*., **104**, 577-584. https://doi.org/10.1016/j.jweia.2012.05.004.

Nozawa, K. and Tamura, T. (2002), “Large eddy simulation of the flow around a low-rise building immersed in a rough-wall turbulent boundary layer", *J. Wind Eng. Ind.Aerod.*, **90**(10), 1151-1162. https://doi.org/10.1016/S0167-6105(02)00228-3.

Pan, Y. and Xiao, Y. (2013). "CFD numerical simulation of tornado wind field and wind loads on structures ", Master's Thesis, Harbin Institute of Technology, Harbin, China.

Wang, F., Tamura, Y. and Yoshida, A. (2014), "Interference effects of a neighboring building on wind loads on scaffolding", *J. Wind Eng. Ind.Aerod.*, **125**, 1-12. https://doi.org/10.1016/j.jweia.2013.11.009.

Wilkins, E.M., Sasaki, Y. and Johnson, H.L. (1975), "Surface friction effects on thermal convection in a rotating fluid: A laboratory simulation", *Mon. Weather Rev*., **103**(4), 305-317.

Xie, Z.N. and Gu, M. (2004), "Mean interference effects among tall buildings", *Eng. Struct*., **26**(9), 1173-1183. https://doi.org/10.1016/j.engstruct.2004.03.007.

Yousef, M.A.A., Selvam, P.R. and Prakash, J. (2018). "A comparison of the forces on dome and prism for straight and tornadic wind using CFD model", *Wind Struct*., **26**(6), 369-382. https://doi.org/10.12989/was.2018.26.6.369.

Zhang, W. and Sarkar, P.P. (2008), "Effects of ground roughness on tornado like vortex using PIV", *In Proceedings of the AAWE Workshop*, U.S.A. August.

FR